Biaxial Stress Behavior of Graphite and Kevlar 49 Fiber/Epoxy Composites and Hybrids

R. F. Foral*
University of Nebraska, Lincoln, Nebraska
and
W. D. Humphrey†
Brunswick Corporation, Lincoln, Nebraska

An experimental investigation was conducted to characterize mechanical behavior of fiber/epoxy composite material under biaxial stress loading. Test specimens were of two types, tubes and domed-end cylindrical pressure vessels, with filament wound [$\pm\alpha$,90] helical/hoop construction. Fiber/epoxy laminates using AS4 graphite fiber, Kevlar 49 fiber, and intraply hybrids combining these fibers were tested. The tubular specimens were subjected to internal pressure with superimposed axial load to determine in-plane mechanical properties. The vessels were tested under internal pressure to correlate the tube data and then burst tested to establish ultimate material strengths. Room temperature creep and recovery tests were included to demonstrate time-dependent behavior.

Introduction

MODERN composites, using continuous fibers in a resin matrix, are important candidate materials in the engineering of energy-efficient structures. In many applications, fiber/matrix materials are lighter, stronger, and possibly cost effective when compared with other materials. Two high-performance fibers of considerable promise are graphite and Kevlar 49. Graphite fiber/epoxy composites typically have high specific strengths and stiffnesses but are somewhat brittle, while Kevlar 49 composites have lower stiffness but exhibit generally greater toughness. Combining more than one type of fibers such as these into a single matrix produces important new materials, the intraply hybrids, with the potential to meet design requirements more efficiently than either single-material composite. As an example of this, Dorey et al.[1] found that graphite/Kevlar 49 hybrids have significantly better impact properties than laminates reinforced with only one of the fiber types.

There is a considerable body of literature on the characterization of intraply hybrids, as exemplified by the extensive bibliographies in available review papers[2,3] and recent test data reports.[4] This paper extends the available work by investigating the biaxial stress behavior of AS4 graphite and Kevlar 49 fiber/epoxy composites and hybrids. The materials are tested in two configurations, tubes and dome-ended cylindrical pressure vessels. Using tubes and vessels rather than coupons minimizes the uncertainties due to the edge effects inherent in coupons. The tubular specimens were subjected to internal pressure with superimposed axial load to determine in-plane mechanical properties. Testing similar to this has been reported previously for single-fiber-type composites.[5,6] The vessels were tested under internal pressure to correlate the tube data and then burst tested to establish ultimate material strengths. In all of the testing the loads were applied incrementally, thus allowing characterization of behavior linearity. Several cycles of loading were applied to test material stability, and material recovery over time was measured after each loading cycle. A room temperature creep test at constant internal pressure was conducted for each specimen.

Presented as Paper 82-0709 at the AIAA/ASME/ASCE/AHS 23rd Structures, Structural Dynamics, and Materials Conference, New Orleans, La., May 10-12, 1982; submitted July 20, 1982; revision received April 20, 1983.

*Professor of Engineering Mechanics.
†Product Development Manager.

Test Specimens

The composites tested in this investigation were made from Kevlar 49 fibers (E. I. du Pont de Nemours & Co.), AS4 graphite fibers (Hercules, Inc.), and LRF-092 epoxy resin matrix (Brunswick Corporation), consisting of diglycidyl ether of bisphenol A epoxy (DGEBA) hardened with nadic methyl anhydride (NMA) per the requirements of Mil-C-47257. The intraply hybrid composites were filament wound with a band having an equal number of spools of four-end Kevlar 49 with 0.352 mm^2 (54.5×10^{-5}in.^{2}) per spool and 6000 tow AS4 graphite with 0.243 mm^2 (37.7×10^{-5}in.^{2}) per spool, producing a 59/41 fiber volume ratio of Kevlar 49 and AS4 graphite. All specimens were cured at a temperature of 141°C (285°F) with slow heating and cooling ramps.

Both tubular and vessel specimens were filament wound in a helical/hoop configuration, [$\pm\alpha$,90,$\pm\alpha$,90] inner to outer. The helical wind angle α was 20.8 deg for the tubes and 11.3 deg for the vessels. Details of the tubular specimens are listed in Table 1, where the designations KT, KAGT, and AGT refer to the Kevlar 49/epoxy, Kevlar 49/AS4 graphite/epoxy, and AS4 graphite/epoxy specimens, respectively. Similarly, the pressure vessel specimens are designated KV, KAGV, and AGV, with vessel details listed in Table 2. As indicated, three replicates of each tubular specimen were tested, with two (one for the Kevlar 49 configuration) replicates of the vessels.

Test Techniques

Tubular Specimens

Figure 1 shows the test setup with a tubular specimen mounted, instrumented, and ready for testing. The tubes were fitted with elastomeric bladders and specially developed wedge-type end fittings[7] to allow simultaneous application of internal pressure and axial load. In the test setup, the specimen was free to expand axially under internal pressure and axial tensile load. Internal pressure was supplied with a 69 MPa (10,000 psi) Enerpac hydraulic hand pump and measured at the specimen with a BLH Electronics 69 MPa

(10,000 psi) general-purpose pressure cell. Axial tensile load was supplied by a 445 kN (100,000 lb) Southwark-Emery universal testing machine, using a special 35.5 kN (8000 lb) low-range dial to measure the loads. Pressure and strain readings were recorded on a B&F Instruments SY161 digital data logger. A load-time record was kept, using a digital chronograph.

Hoop and axial specimen strains were measured at mid-cylinder at three evenly spaced circumferential locations. At each location, electrical resistance strain gages (Micro-Measurements EA-06-250BG-120), aligned in the hoop and axial directions, were bonded directly to the specimen surface, which was carefully smoothed. Temperature compensation was provided with duplicate strain gages mounted on an unloaded specimen identical to the specimen being tested. Corrections for transverse gage sensitivity were applied in interpreting all strain gage readings.

At each strain gage location, axially aligned special strain transducers[8] were used. The transducers, visible in Fig. 1, consist of strain-gaged curved beams contacting the composite point to point over a 50.8 mm (2 in.) gage length. In this manner, resin crazing (visually detectable cracking) in the outer hoop layers, which can damage directly applied axial gages, is bridged. When compared with the axial strain gages, the transducers were found[8] to be very accurate and more reliable. For this reason, strain readings from the transducers and the directly applied hoop gages are used in this paper.

The test section of the tubular specimens is nominally 17.8 cm (7 in.) in length. Since specimen proportions can have important effects on results, a finite element stress-strain analysis of the tube has been conducted. The analysis indicated that sufficient length has been provided so that the central section is strained uniformly, free from bending-extension coupling, and end restraint and thick wall effects.

Figure 2 plots a typical loading curve, hoop vs axial normal running load, where at increasing values of internal pressure (indicated by the circles) increments of axial load are applied. An increment of internal pressure Δp produces axial and hoop running load increments ΔN_x^p and ΔN_θ^p that are related to the axial and hoop strain increments $\Delta\epsilon_x^p$ and $\Delta\epsilon_\theta^p$ by

$$\Delta N_x^p = \Delta p \cdot r/2 = A_{11}\Delta\epsilon_x^p + A_{12}\Delta\epsilon_\theta^p \quad (1)$$

$$\Delta N_\theta^p = \Delta p \cdot r = A_{21}\Delta\epsilon_x^p + A_{22}\Delta\epsilon_\theta^p \quad (2)$$

Table 1 Tubular specimen details (helical wind angle $\alpha = 20.8$ deg, 70.6 mm i.d.)

	KT	KAGT	AGT
Number of specimens	3	3	3
Fiber thickness, mm		K/AG	
Helical	0.663	0.300/0.208	0.549
Hoop	0.859	0.460/0.318	0.721
Avg laminate thickness, mm	2.64	2.46	2.21
Fiber volume ratio, %	58	52	57

Conversion factor: 1 mm = 0.03937 in.

Table 2 Pressure vessel specimen details (helical wind angle $\alpha = 11.3$ deg, 164 mm i.d.)

	KV	KAGV	AGV
Number of specimens	1	2	2
Fiber thickness, mm		K/AG	
Helical	0.678	0.452/0.312	0.625
Hoop	1.074	0.716/0.495	0.991
Avg laminate thickness, mm	2.76	3.48	3.45
Fiber volume ratio, %	63	57	47

Conversion factor: 1 mm = 0.03937 in.

where r is the tube radius and A_{11}, A_{12}, A_{21}, and A_{22} are elements of the stiffness matrix[9] of the material. An increment of axial load ΔT produces axial and hoop running load increments ΔN_x^T and ΔN_θ^T that are related to the axial and hoop strain increments $\Delta\epsilon_x^T$ and $\Delta\epsilon_\theta^T$ by

$$\Delta N_x^T = \Delta T/2\pi r = A_{11}\Delta\epsilon_x^T + A_{12}\Delta\epsilon_\theta^T \quad (3)$$

$$\Delta N_\theta^T = 0 = A_{21}\Delta\epsilon_x^T + A_{22}\Delta\epsilon_\theta^T \quad (4)$$

Equations (1-4) allow evaluation of the stiffness matrix once the load and strain increments are determined in test. Referring to the loading curve in Fig. 2, an increment of pressure and of axial load is applied at each pressure level (indicated by the circles). Thus, a sequence of evaluations of the stiffness matrix is allowed and linearity of behavior can be characterized. The procedure allows determination of the four matrix elements without recourse to symmetry assumptions. Thus, stiffness matrix symmetry, and all that it implies, can be checked.

A typical tubular specimen test sequence involved incremental load applications such as shown in Fig. 2, repeated over several cycles of loading to test material stability. Considerable care was taken to conduct the loadings quickly and smoothly to minimize the effects of material creep at the constant pressure hold. Each load change was timed and an accurate load-time record kept. Material strain recovery over time was measured after each loading cycle. A room temperature creep test at constant internal pressure was conducted for each specimen.

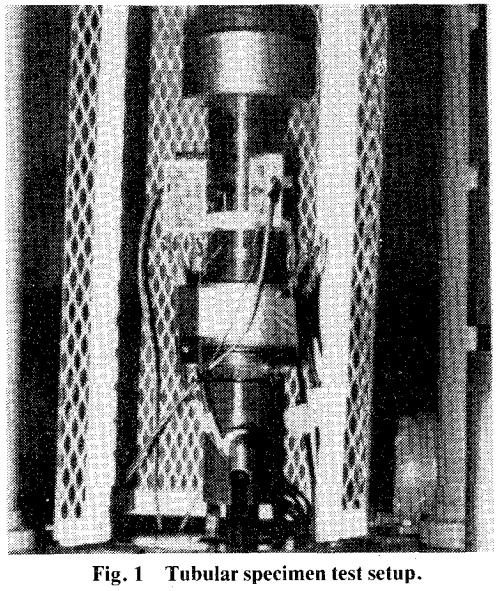

Fig. 1 Tubular specimen test setup.

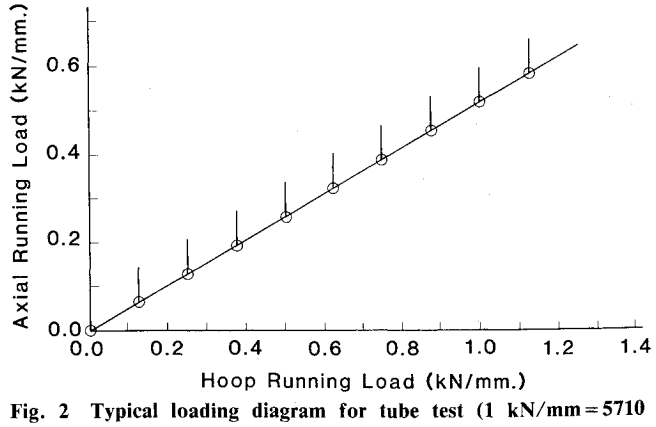

Fig. 2 Typical loading diagram for tube test (1 kN/mm = 5710 lb/in.)

Pressure Vessel Specimens

The pressure vessel specimens described in Table 2 were subjected only to internal pressurization. The AS4 graphite/epoxy vessels (AGV) were fabricated late in the program and were subjected only to proof pressurization and bursts tests. The Kevlar 49/epoxy vessel (KV) and the hybrid vessels (KAGV) were subjected to a special test sequence, as described below.

Figure 3 shows one of the hybrid vessels KAGV mounted, instrumented, and ready for test. The pressurization system, strain and pressure measurement, and data recording techniques were exactly like those previously described for the tubular specimens. A typical KV and KAGV vessel test sequence involved incremental pressurization over several cycles, with strain recovery over time measured after each pressurization cycle. A room temperature creep test was conducted at constant internal pressure. Finally, all vessels were burst tested.

Results and Discussion

Laminate Stiffness Properties

Figures 4-6 plot the laminate performance of tubular specimens KT, KAGT, and AGT, respectively.

Pressure-strain performance of the tubes is shown in Figs. 4a, 5a, and 6a where test readings are indicated by the symbols and the solid lines connect the average strain readings for each tube. As can be seen, the pressure-strain plots are linear and repeatable, cycle to cycle and specimen to specimen. For each tube, audible resin crazing occurred during the first cycle, after which the tubes were very quiet under load, provided the load did not exceed a previously attained value.

To depict laminate stiffness properties, stiffness coefficients $\bar{A}_{ij}$ are introduced, where

$$\bar{A}_{ij} = A_{ij}/h \qquad (i,j=1,2) \tag{5}$$

and h is the laminate thickness. Figures 4b, 5b, and 6b show plots of the stiffness coefficients vs internal pressure over five loading cycles. In these figures, the symbols plot the stiffness coefficients calculated at each pressure level using Eqs. (1-4).

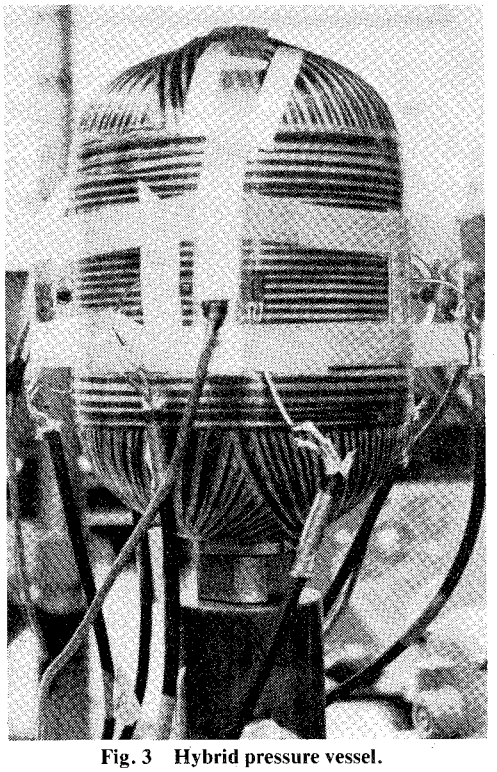

Fig. 3 Hybrid pressure vessel.

The solid lines connect the symbols for each tube over the pressure range. Stiffness matrix symmetry was assumed for the Kevlar material; comparing $\bar{A}_{12}(+)$ and $\bar{A}_{21}(x)$ values for the other materials indicates the symmetry assumption is valid, especially in view of the relatively small numerical value of these coefficients.

For all of the materials, stiffness coefficient repeatability is good, cycle to cycle and specimen to specimen. The stiffness coefficients are essentially constant over the pressure range for each cycle. There is a trend of variation in the values: the $\bar{A}_{22}$ and $\bar{A}_{11}$ values increase slightly and the $\bar{A}_{12}$ and $\bar{A}_{21}$ values decrease slightly with increasing pressure. The basic data, not given here, reflect this—the strain increment magnitudes show tendencies to decrease with increasing pressure, especially in the increments due to axial load. If this apparent stiffening effect is caused by material creep, it can be eliminated by using only the starting values of the stiffness coefficients. These are calculated at a base condition of zero internal pressure for which there is no creep. Creep behavior of the materials will be demonstrated later in the paper.

Material creep has the largest potential effect on the small hoop strain change $\Delta\epsilon_\theta^T$ due to the axial load increment. At constant internal pressure, application of an axial load increment causes a small negative hoop strain change, which can be affected, or even eliminated, by continuing creep due to the internal pressure. When material creep has an important influence as with the KT specimens, the $\Delta\epsilon_\theta^T$ strain increment should be neglected and the stiffness matrix symmetry assumed. When this is done with the KAGT and AGT data, calculations show little change in $\bar{A}_{11}$ and $\bar{A}_{22}$, while $\bar{A}_{12}$ closely follows the $\bar{A}_{12}$ calculated without the symmetry assumption.

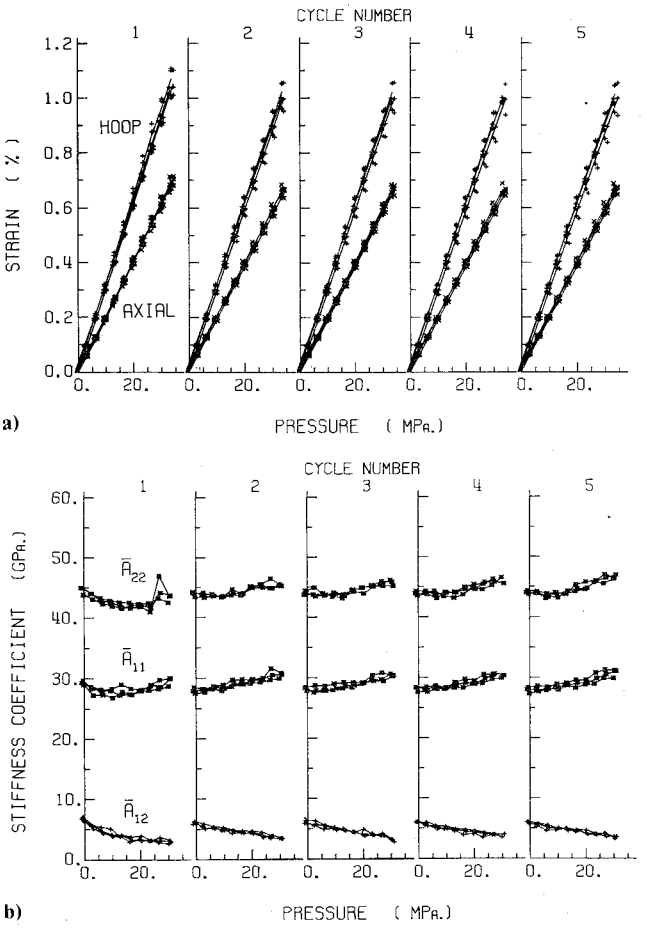

Fig. 4 Strain response (a) and stiffness coefficients (b) for tubular specimens KT (1 MPa = 145 psi).

In Fig. 7, the average values (over a cycle) of the stiffness coefficients for each tube are plotted vs cycle number. The solid lines connect the average values of the plotted points. The plots show good repeatability, specimen to specimen and cycle to cycle. Interestingly, and for unknown reasons, the $\bar{A}_{12}$ and $\bar{A}_{21}$ averages for AGT are distinctly different, although nearly equal. The overall average of the stiffness coefficient values plotted in Fig. 7 are listed in Table 3. The listed values for KT and AGT are combined according to the rule of mixtures[5] to calculate predicted hybrid values, using the known 59/41 Kevlar 49/graphite fiber ratio. The percent difference values listed in Table 3 are comparable to those obtained by Chamis et al.[5] for coupons and indicate a good utilization of the constituents in the hybrid.

Knowing the stiffness coefficients from the tube tests, the ply properties can be determined using classical lamination theory.[9] The analysis involves assuming a sequence of longitudinal modulus values for the ply and allowing for some experimental error. Ply properties resulting from this procedure are listed in Table 4. This is one set of the several possible combinations of ply properties that could produce similar laminate behavior. Further study of the influence of individual ply properties on laminate behavior would be of interest.

Pressure-strain plots for cyclic testing of the pressure vessels were very similar to the tubular specimen plots (Figs. 4a, 5a, 6a) and thus are not presented here. Peak cyclic pressures and corresponding average strains for the vessels are listed in Table 5, along with theoretical predictions. These were obtained using the lamination theory with the ply properties of Table 4 modified for the fiber volume ratio. The results show that the ply properties determined from the tube tests can be used to predict pressure vessel strains with reasonable accuracy.

Laminate Strength

Pressure vessel burst tests produced midcylinder failures in all vessels at the internal pressure values listed in Table 5. Comparative vessel performance is evaluated in Table 5 using the efficiency parameter $p_B V/W$ (burst pressure times enclosed volume divided by composite weight). Although only one Kevlar 49/epoxy vessel is tested here, the $p_B V/W$ value shown is typical of numerous tests from other programs. Based on these limited data, an apparent synergism in performance emerges—the hybrid vessel has a higher efficiency, as measured by $p_B V/W$, than either constituent vessel.

Assuming linear behavior to fracture, projected burst strains are 1.97, 1.76, and 1.42% for KV, KAGV, and AGV, respectively. The burst strain values for KV and AGV agree very closely with the fiber elongation data for Kevlar 49 and AS4 graphite fibers, indicating that maximum fiber strain is a good failure criterion for the vessels. The KAGV value of 1.76% indicates a synergistic effect—the AS4 graphite fibers attained a higher strain level in the hybrid laminate than in the single-fiber of laminate.

Time-Dependent Behavior

After each loading cycle, hoop and axial strains were measured vs time from load removal to demonstrate material recovery behavior. Hoop recovery data for typical tubes KT, KAGT, and AGT are plotted in Fig. 8. The specimens had been allowed to stabilize and the strain gages had been set to zero before each load application cycle. Residual strain continues to accumulate at about 100 μm per cycle for KT while the AGT specimen stabilizes after the first cycle, as does

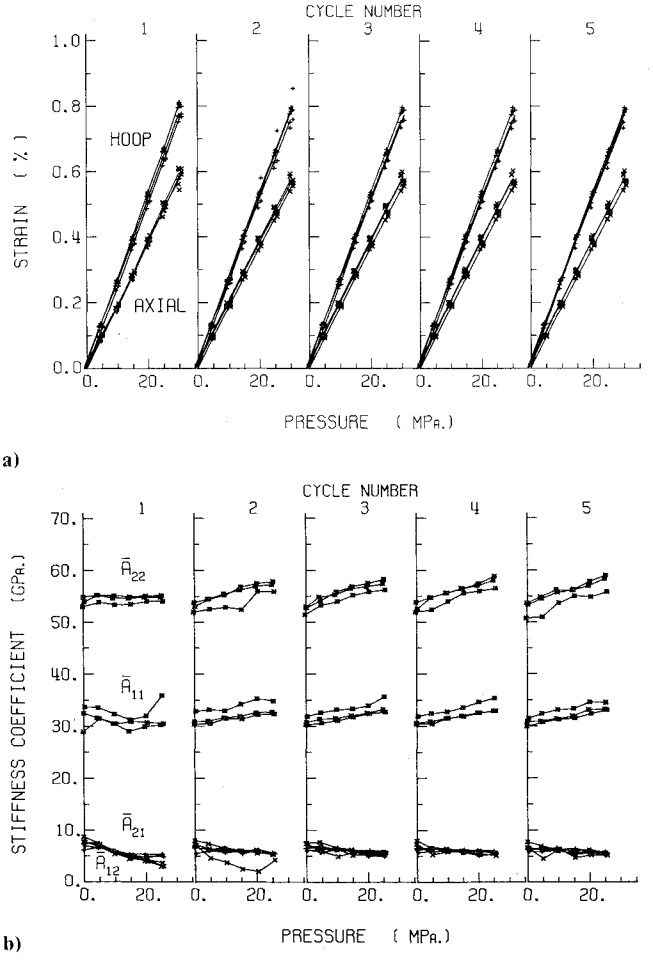

Fig. 5 Strain response (a) and stiffness coefficients (b) for tubular specimens KAGT (1 MPa = 145 psi).

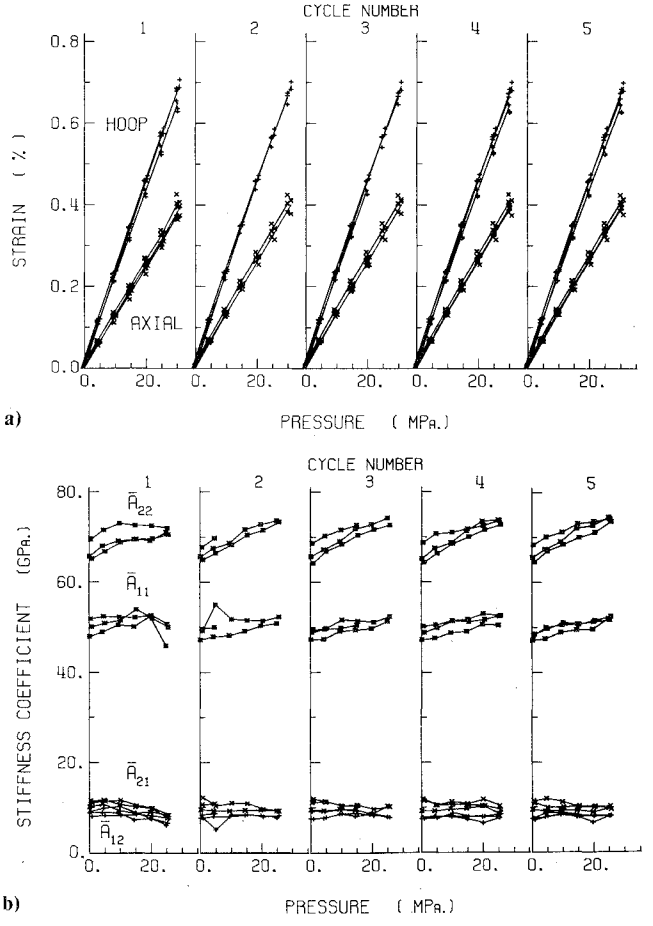

Fig. 6 Strain response (a) and stiffness coefficients (b) for tubular specimens AGT (1 MPa = 145 psi).

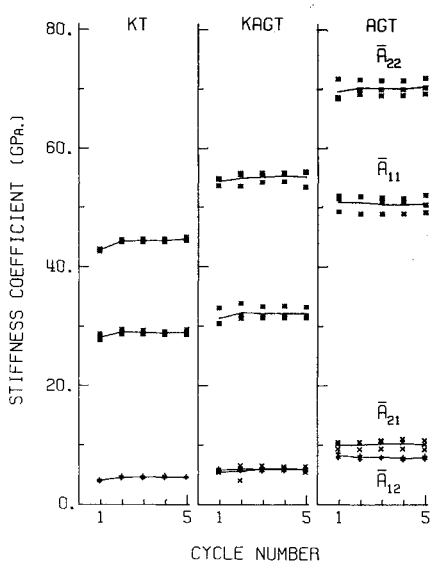

Fig. 7 Average stiffness coefficients for all tubular specimens (1 GPa = 145 × 10³ psi).

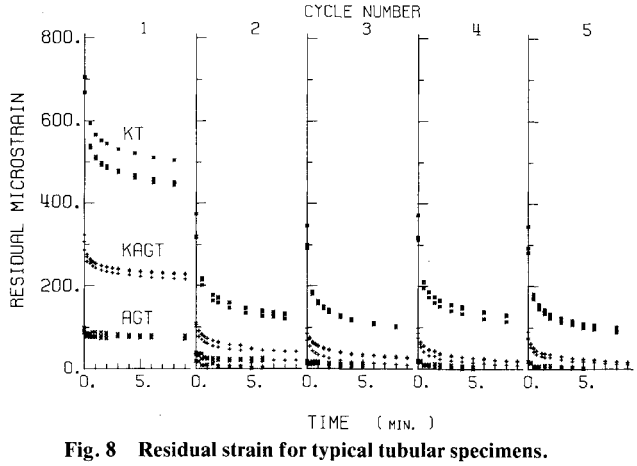

Fig. 8 Residual strain for typical tubular specimens.

Table 3 Average laminate stiffness coefficients of tubes, GPa

Coefficient	KT	KAGT			AGT
		Test	Theory[a]	%	
$\bar{A}_{11}$	28.8	32.1	37.8	15.0	50.7
$\bar{A}_{22}$	44.1	55.0	54.8	0.0	70.1
$\bar{A}_{12}$	4.52	6.38	5.94	7.4	8.00

[a] Rule of mixtures. Conversion factor: 1 GPa = 145 · 10³ psi.

Table 4 Compatible unidirectional ply properties

Property	Material K	KAG	AG
Modulus, GPa			
Longitudinal	73.8	86.2	124.1
Transverse	4.1	6.2	10.3
Shear	1.4	2.8	4.8
Poisson's ratio	0.25	0.25	0.2

Conversion factor: 1 GPa = 145 · 10³ psi.

KAGT to a lesser extent. Axial recovery data are similar to the hoop data. Strain recovery data for the vessels are similar to tube data, and are not presented here.

All creep data reported are hoop fiber creep produced in room temperature tests at constant internal pressure. Axial creep data were recorded, but, being similar to the hoop data,

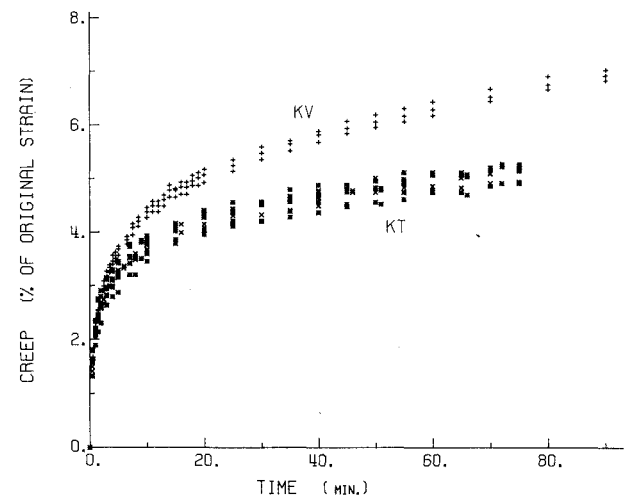

Fig. 9 Creep behavior for Kevlar 49/epoxy specimens.

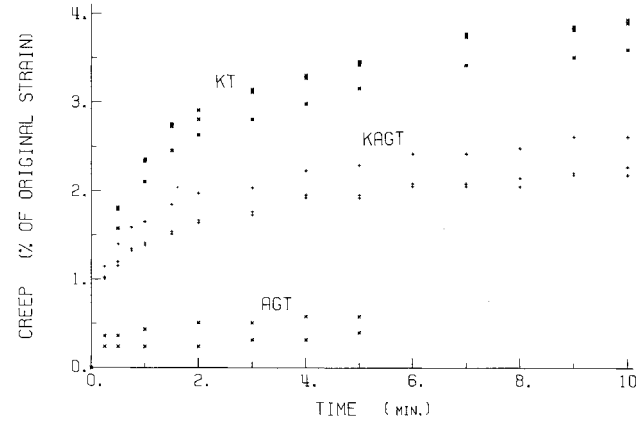

Fig. 10 Creep behavior for typical tubular specimens.

Table 5 Pressure vessel performance

	KV	KAGV	AGV
Cyclic pressure, MPa	17.2	20.7	22.9[a]
Cyclic strain, %			
Hoop (test/theory[b])	1.09/1.00	0.83/0.80	0.79/0.79
Axial (test/theory[b])	0.80/0.77	0.62/0.60	0.59/0.58
Burst pressure, MPa	31.2	43.4	41.0
		44.1	41.2
$p_B V/W$, km	24.9	28.2	24.9
		28.4	25.1

[a] Proof pressure only. [b] Classical lamination theory. Conversion factors: 1 MPa = 145 psi, 1 km = 39.37 × 10³ in.

are not reported here. Creep is plotted as percent of original strain, the initial strain value recorded when the creep pressure level was first reached. The creep data are represented analytically by

$$\%\epsilon = A + B \cdot \ln(t) \tag{6}$$

where A and B are constants determined by a least mean squares data-fitting routine and t is the time in minutes.

Creep data for the Kevlar 49 pressure vessel and tubes are plotted in Fig. 9. Each of the three tubular specimens was tested at 20.7 MPa (3000 psi) internal pressure, while the vessel was tested at 13.8 MPa (2000 psi). Even though these are short-term tests, creep behavior is similar to that reported previously for Kevlar 49 fibers[10] and unidirectional composites.[10,11] From the data, it appears that creep in Kevlar 49 could be a significant factor in design considerations.

Table 6 Tube creep data

	KT	KAGT	AGT
Pressure, MPa	20.7	31.0	31.0
Initial strain, %	0.62	0.79	0.66
Percent of burst, %	31	45	46
$\%\epsilon = A + B \cdot \ln(t)$			
A	2.27	1.51	—
B	0.68	0.36	—
Correlation[a]	0.95	0.87	—

[a] Values near unity indicate a good fit. Conversion factor: 1 MPa = 145 psi.

Table 7 Vessel creep data

	KV	KAGV
Pressure, MPa	13.8	20.7
Initial strain, %	0.88	0.83
Percent of burst, %	44	47
$\%\epsilon = A + B \cdot \ln(t)$		
A	2.07	1.07
B	1.02	0.41
Correlation[a]	0.99	0.96

[a] Values near unity indicate a good fit. Conversion factor: 1 MPa = 145 psi,

Creep data for all tubular specimens are summarized in Table 6 and comparatively plotted for typical specimens in Fig. 10. Table 7 summarizes creep data for the vessel specimens. The vessel creep data are similar to the tube data and are not plotted. From the data, it is apparent that Kevlar 49 vessels and tubes show the highest creep strains, while the graphite specimens show little tendency to creep. Adding graphite to Kevlar 49 produces a hybrid with significantly modified creep tendencies.

Conclusions

Major findings of this investigation include:

1) An experimental technique for characterizing advanced composite materials under biaxial stress has been developed.

2) Laminated fiber/epoxy composites of Kevlar 49, AS4 graphite, and intraply hybrids of these materials have been tested in tubular and pressure vessel configurations.

3) Basic mechanical properties and behavior of the selected materials have been characterized.

4) The intraply laminates tested showed effective utilization of constituent properties.

Acknowledgment

This program operated under the Cooperative Support Agreement between Brunswick Corporation and the University of Nebraska—Lincoln as part of Brunswick's ongoing IR&D effort. F. Steele of Brunswick provided invaluable contributions in specimen fabrication and expediting. Testing was performed by P. Grosserode, J. Wilson, D. Foral, and B. Fix.

References

[1] Dorey, G., Sidey, G. R., and Hutchings, J., "Impact Properties of Carbon Fibre/Kevlar 49 Fibre Hybrid Composites," *Composites*, Vol. 9, No. 1, Jan. 1978, pp. 25-32.

[2] Short, D. and Summerscales, J., "Hybrids—a Review, Part I: Techniques, Design and Construction," *Composites*, Vol. 10, No. 4, Oct. 1979, pp. 215-221.

[3] Short, D. and Summerscales, J., "Hybrids—a Review, Part 2: Physical Properties," *Composites*, Vol. 11, No. 1, Jan. 1980, pp. 33-38.

[4] Chamis, C. C., Lark, R. F., and Sinclair, J. H., "Mechanical Property Characterization of Intraply Hybrid Composites," *Test Methods and Design Allowables for Fibrous Composites*, ASTM STP 734, American Society for Testing and Materials, Philadelphia, 1981, pp. 261-280.

[5] Bert, C. W. and Guess, T. R., "Mechanical Behavior of Carbon/Carbon Filamentary Composites," *Composite Materials: Testing and Design (Second Conference)*. ASTM STP 497, American Society for Testing and Materials, Philadelphia, 1972, pp. 89-106.

[6] Guess, T. R. and Gerstle, F. P. Jr., "Deformation and Fracture of Resin Matrix Composites in Combined Stress States," *Journal of Composite Materials*, Vol. 11, No. 2, 1977, pp. 147-163.

[7] Cederberg, A. R., Foral, R. F., and Reiners, A. G., "Mechanical Behavior Testing of Composite Tubular Specimens," *Proceedings, SESA 1983 Spring Conference*, Society for Experimental Stress Analysis, May 15-19, 1983, Cleveland, Ohio, pp. 284-290.

[8] Cederberg, A. R. and Foral, R. F., "A Strain Gage Transducer for Measuring Strains in Composite Materials," *Proceedings of the 1982 Joint Conference on Experimental Mechanics*, Society for Experimental Stress Analysis-Japan Society of Mechanical Engineers, 1982, Pt. II, pp. 1096-1101; also *Experimental Techniques*, Vol. 7, No. 5, 1983, pp. 22-25.

[9] Jones, R. M., *Mechanics of Composite Materials*, Scripta Book Co., Washington, D.C., 1975.

[10] *Kevlar 49 Data Manual*, E. I. du Pont de Nemours & Company, Wilmington, Del.

[11] Ericksen, R. H., "Room Temperature Creep of Kevlar 49/Epoxy Composites," *Composites*, Vol. 7, No. 3, July 1976, pp. 189-194.